JOURNAL OF MATERIALS SCIENCE 5 (1970) 856-861

Fatigue of Mg_3Cd

Part 2 *Fractographic Aspects*

R. S. WHITEHEAD, F. W. NOBLE
Department of Metallurgy and Materials Science, University of Liverpool, Liverpool, UK

Scanning electron microscopy has been used to study the fracture surface characteristics of single crystals and polycrystals of Mg_3Cd after fatigue failure. Certain aspects of the crack propagation mode are attributed to the crystallography of the hexagonal structure of Mg_3Cd. The transition from crystallographic crack growth, to growth normal to the stress axis is discussed in terms of the slip character of ordered and disordered polycrystalline Mg_3Cd.

1. Introduction

Although the fatigue properties of many hexagonal metals have been fairly extensively investigated, the crystallographic aspects of crack propagation in these materials has largely been ignored. The properties of both ordered and disordered Mg_3Cd are well suited to such a fractographic study since crystals which will deform chiefly by either basal slip or prismatic slip can be prepared in the required orientations for both states of order. A further advantage associated with this material is its disinclination to twin in the ordered and the disordered condition so that the fracture process is free from the complicating factors of slip-twin interactions and crack nucleation along twin-matrix interfaces [1, 2]. The present work is, therefore, concerned primarily with the fractographic aspects of Mg_3Cd as a hexagonal alloy, rather than in terms of variation of properties with degree of order, though in the case of the polycrystalline material attention will be paid to the latter aspect.

2. Experimental Details

The experimental procedure with respect to specimen preparation and testing has already been described in part 1. The fracture surfaces of fatigued specimens were examined using a Cambridge Stereoscan electron microscope, supplemented by optical microscopy. For the purpose of examining partially failed specimens the fatigue machine was fitted with a device which automatically stopped the test when a preselected specimen elongation occurred. All fractographic observations were made on specimens fatigued in air at room temperature.

3. Experimental Results

3.1. Polycrystalline Specimens

Fig. 1 shows a composite picture of a fatigue crack in a specimen of ordered Mg_3Cd fatigued at a stress of $\pm$ 7.4 kg mm^{-2} for 1.35 $\times$ 10^5 cycles. Crack initiation appears to have occurred in the heavily striated grain at the specimen edge and, in the early stages, crack growth is predominantly along the operative slip planes in the material. In the later stages, towards the tip of the crack, the path of the crack becomes noticeably non-crystallographic and is at 90° to the stress axis indicating the onset of stage II crack propagation [3]. The general features of crack growth in disordered Mg_3Cd appeared to be very similar to the ordered (with possibly more grain boundary cracks in the disordered alloy) and close to the tips of stage II fatigue cracks, the slip morphology was similar for both states of order.

The transition from stage I, crystallographic propagation to stage II propagation at right-angles to the stress axis was visible macroscopically on the fracture surfaces of broken specimens, the region of stage I growth being heavily faceted in comparison with the region of stage II growth in both ordered and disordered Mg_3Cd. Fig. 2 shows the percentage of the fracture surface area associated with stage I growth as a function of stress-amplitude for both ordered and disordered material. Although there is some scatter, particularly at higher stresses, close to the fatigue

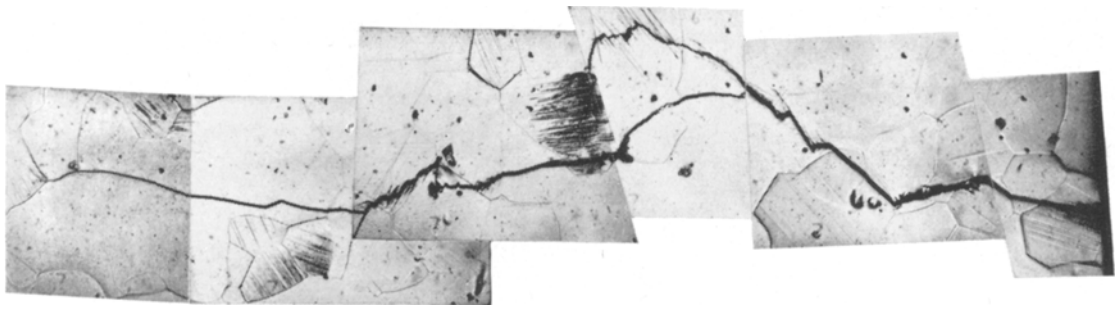

Figure 1 Fatigue crack in ordered Mg_3Cd fatigued at $\pm$ 7.4 kg mm^{-2} for 1.35 $\times$ 10^5 cycles ($\times$ 350).

limit the ordered specimens exhibit 90% crystallographic growth, compared with about 70% for the disordered, and at higher stresses there appears generally to be a greater amount of stage I growth in the ordered specimens. These results are similar to those of Williams and Smith [4] on β-brass though neither line appears to extrapolate to 100% crystallographic growth at zero stress as did the β-brass results. This implies that, unlike β-brass, the transition to stage II growth in Mg_3Cd does not occur simply when the stress on the uncracked section reaches a constant critical value.

During stage II propagation, well defined striations were observed on the fracture surfaces the form and intensity of which were strongly dependent on the orientation of individual grains. A composite photograph of the fracture surface associated with stage II propagation in a high stress test on an ordered polycrystalline specimen is shown in fig. 3.

3.2. Single Crystals

Single crystal specimens oriented for prismatic slip had orientations such that the basal plane lay along the stress axis and either one of the $\{1\bar{1}00\}$ or $\{11\bar{2}0\}$ prism planes lay approximately at 90° to the stress axis. Similar specimens were used in both ordered and disordered conditions and, as the crystallographic aspects of crack growth were virtually the same in both conditions, attention will be concentrated on the results for a single ordered specimen fatigued at an alternating resolved shear stress of τ_p = $\pm$ 1.9 kg mm^{-2} for 1.1 $\times$ 10^5 cycles, which showed off these aspects to best advantage.

Fig. 4a shows a low magnification view of the fracture surface of this specimen which, in spite of the deceptive perspective of the picture, is at 90° to the stress axis, and parallel to a $\{100\}\bar{1}$

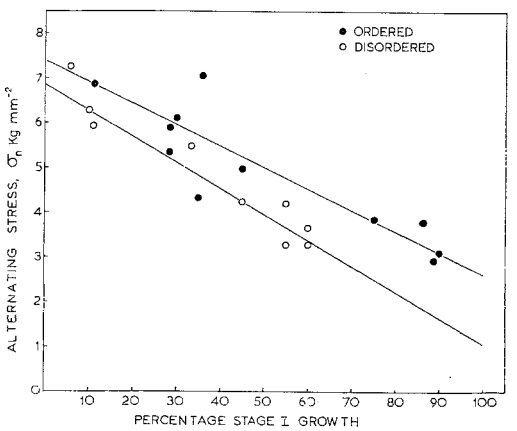

Figure 2 Alternating stress, σ_n, vs. percentage stage I crack growth.

prism plane. A schematic diagram of this fracture surface is shown in fig. 4b. The crack started to the left of point "A" at the top of the smooth "V" shaped region, and propagated in the direction A-B. Final failure in these specimens frequently involved cleavage on the basal plane in spite of its "unstressed" position and the edge A-B is in fact the trace of the basal plane upon which this specimen cleaved eventually longitudinally.

While the "V" shaped region was relatively featureless, the remainder of the fracture surface was heavily covered with fatigue striations and with ridges running parallel to the basal plane trace, i.e. parallel to A-B. Fig. 5 shows a high magnification view of one of these ridges, the edges are parallel to the basal plane – the striations to the intersection of the two most heavily stressed prism planes with the fracture surface, i.e. parallel to $<0001>$. Towards the end of the crack propagation process the ridge formations

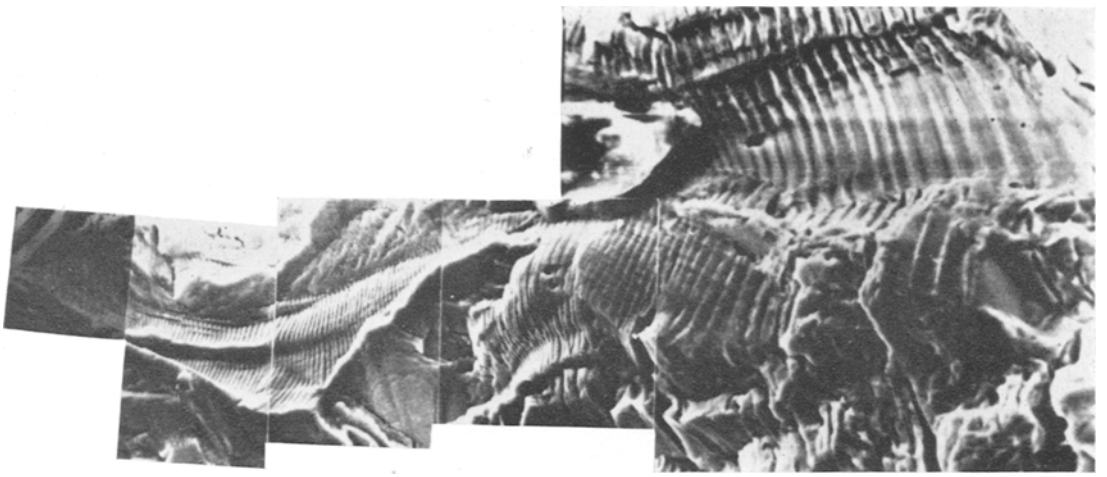

Figure 3 Composite stereoscan picture of fracture surface associated with stage II growth in ordered polycrystalline Mg_3Cd polycrystal (× 650).

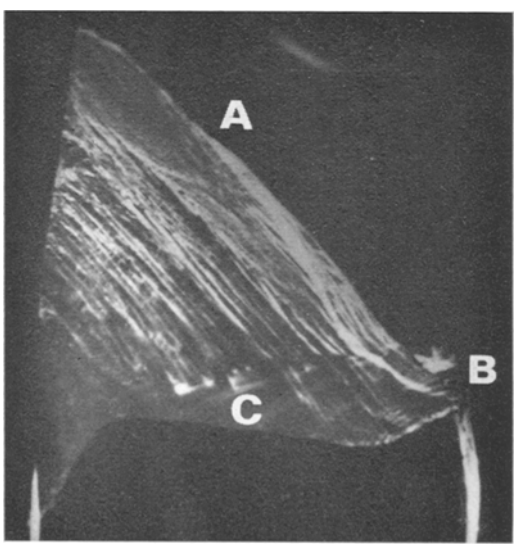

Figure 4 (a) General view of fracture surface of an ordered single crystal oriented for prismatic slip, failed after 1.1×10^5 cycles at $\pm$ 1.9 kg mm^{-2} alternating shear stress (× 24).

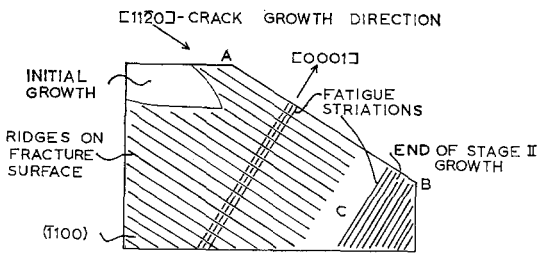

Figure 4 (b) Schematic diagram of fracture surface shown in fig. 4a.

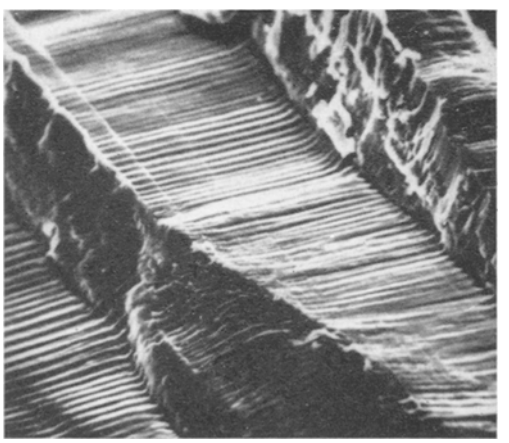

Figure 5 Ridge on fracture surface exhibiting well defined fatigue striations parallel to <0001> (× 400).

tend to peter out as shown in fig. 6, which is taken from the area denoted by point "C" in fig. 4. A schematic diagram of the crystallography associated with this crack propagation behaviour is shown in fig. 7. The profile of the fatigue striations in the region of point "C" is shown in fig. 8 and indicates a saw-tooth configuration, apparently with the faces of the striations parallel to the two prism planes symmetrically placed at 60° to the fracture face. The main difference between the behaviour of ordered and disordered crystals was in the greater distortion of the fracture faces of the latter crystals, possibly due to the higher applied stresses.

Crystals oriented for basal slip showed

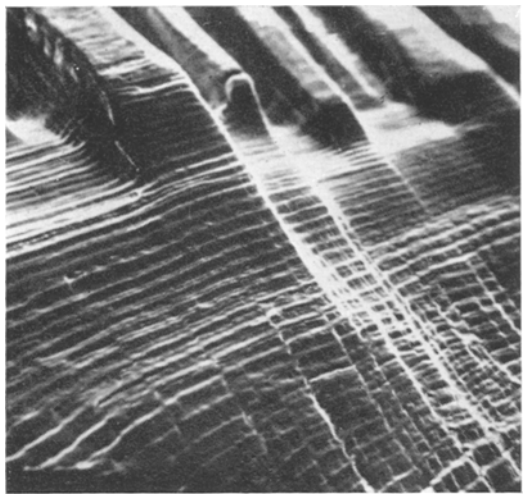

Figure 6 Change in fracture surface morphology towards the end of crack propagation. The sides of the ridges at the top of picture are parallel to the basal plane (× 150).

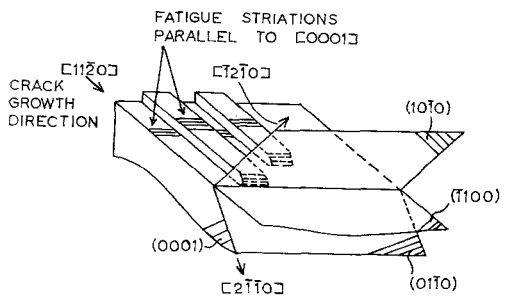

Figure 7 Schematic diagram of crystallography associated with crack growth parallel to a prism plane.

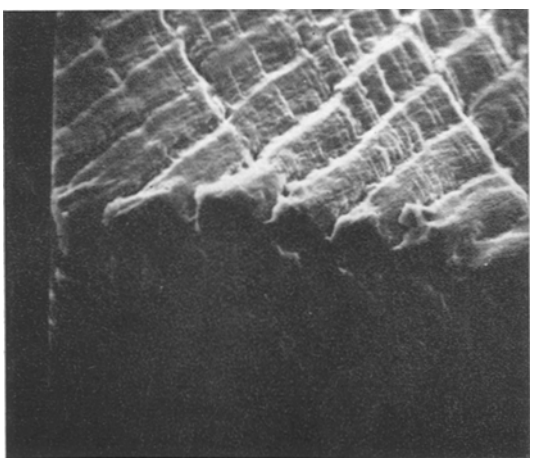

Figure 8 Sawtooth profile of striations near the end of stage II propagation in specimen oriented for prismatic slip (× 450).

different fracture characteristics to the above crystals, depending upon state of order. The path taken by a propagating fatigue crack in a disordered crystal oriented for basal slip is shown in fig. 9. The departure of the crack from propagation along the basal plane appears to occur almost immediately, but is very gradual. Fractographs of a similar specimen which had failed reveal a very small, featureless stage I growth region followed by a striated fracture surface, fig. 10.

Ordered crystals oriented for basal slip showed no extensive fatigue crack propagation, but invariably failed by basal cleavage after an initial period of fatigue crack growth. Fig. 11 shows the fracture surface associated with this behaviour, the crack having propagated from the top edge over about 25% of the fracture face before cleavage occurred.

4. Discussion

Although the slip traces on ordered specimens show evidence of prolific cross-slip, in the sense that segments of a given slip band may alternate between basal and prism planes, the frequent cross-slip of individual dislocations will be restricted, due to the formation (at least on the basal plane) [5, 6] of superlattice dislocations. In contrast, in spite of the higher stress required for prismatic slip in disordered Mg_3Cd, cross-slip of individual dislocations between basal and prism planes should be relatively easy, provided the dislocations are not extended appreciably on the basal planes. If this distinction between the two states of order is valid the disordered material should show less reversibility of slip than the ordered, a property which, according to Wells [7] should favour an earlier transition from stage I to stage II crack growth, as observed here.

The $<11\bar{2}0>$ slip directions in which slip in both ordered and disordered Mg_3Cd almost invariably occurs are, of course, co-planar and this property imposes restrictions on the deformation processes possible at the crack tip, which are not encountered in fcc materials. In the situation illustrated in fig. 9 for example, in which the crystal is deforming by basal slip, crack growth at a finite angle to the basal plane is associated with considerable crystallographic asymmetry. Consequently, the "sawtooth" configuration of {111} slip planes, which Hertzberg [8] identified with crystallographic striation formation on the fracture surfaces of fcc metals, has no analogue

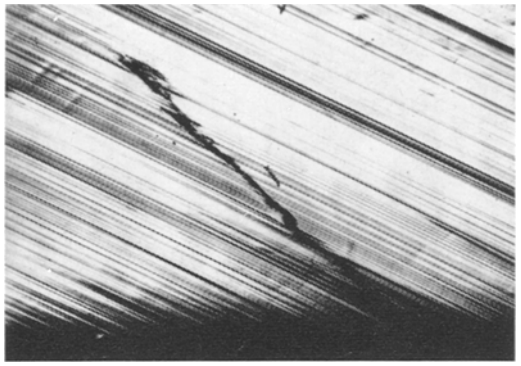

Figure 9 Crack propagation in disordered crystal oriented for basal slip (× 45).

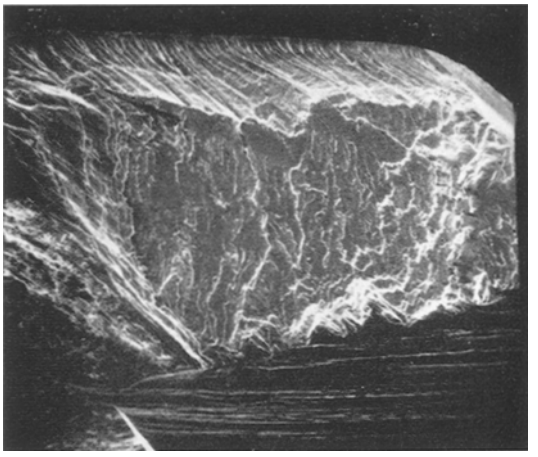

Figure 11 Fracture surface of ordered crystal oriented for basal slip, which failed after 3×10^4 cycles (× 35).

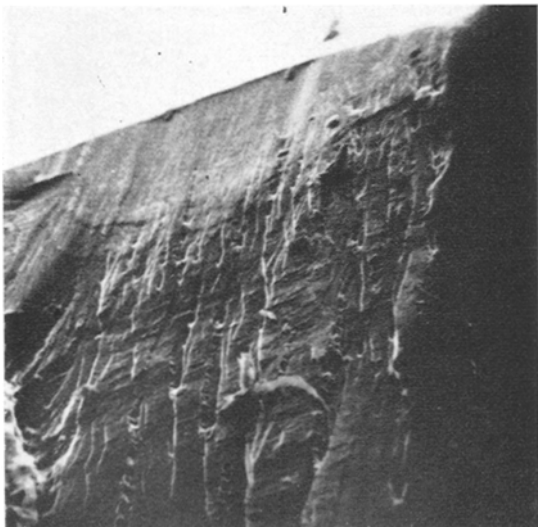

Figure 10 Fracture surface associated with early stages of crack propagation in a disordered crystal oriented for basal slip (× 75).

in the crystal orientation in question (assuming no appreciable second order pyramidal slip). Similarly the crystallographic mechanism proposed by Neumann [9] does not appear to be applicable to the formation of striations, such as those in fig. 10, unless non-basal slip vectors become operative to provide an intersecting slip system.

The most probable mechanism for the striation formation, therefore, would appear to be Laird's [10] plastic blunting model, though here again the restricted slip systems are a complicating factor. For example, the crack blunting process on the tensile cycle will involve shear on the basal plane in opposite senses on either side of the plane of fracture, in one case in the opposite direction to the resolved shear stress due to the applied stress. At best the situation will approximate to the asymmetrical fcc case discussed by Laird, and the "double ear" configuration associated with the crack tip should be uneven; though there was no evidence for such asymmetry on the matching fracture faces.

The crystallography involved in crack propagation in the crystals oriented for prismatic slip, fig. 7, approximates much more closely to the idealised fcc situation as two $\{1\bar{1}00\}$ prism planes are symmetrically disposed at $\pm$ 60° to the crack propagation plane. The geometry is not perfectly analogous, however, since each plane contains only a single slip vector which will restrict the deformation at the crack tip. The crack initially appears to grow without forming well defined striations until the "V" shaped configuration near point "A" in fig. 4 is achieved – the most rapid growth having occurred in the $<11\bar{2}0>$ direction. The transition of growth mode which then occurs is presumably due to the increased stress on the uncracked section. Because of the single slip directions associated with the slip planes, upon which the deformation at the crack tip must be concentrated, the crack apparently prefers to propagate on a segmented front, each segment propagating in the direction of the projection of the slip vectors on the fracture surface. This mode of propagation will inevitably involve large shear stresses between each segment, as they obviously cannot propagate independently, and it is suggested that the

ridges running at right angles to the striations, fig. 5, are due to shear on the basal planes lying along the stress axis. This rather peculiar fracture surface configuration is not, however, exclusive to cph materials since Hoepner [11] has reported a rather similar topography in coarse grained polycrystalline copper.

Although the final stages of crack growth in prismatic slip specimens are not as strongly crystallographic, the profile of the striations observed in this region, fig. 8, appear to be very much of the sawtooth variety being parallel to the intersecting $\{1\bar{1}00\}$ planes.

References

1. R. W. ARMSTRONG and G. T. HORNE, *J. Inst. Metals* **91** (1962) 311.
2. C. J. BEEVERS and M. D. HALLIDAY, *Met. Sci. J.* **3** (1969) 74.
3. P. J. E. FORSYTHE, *Proc. Crack Propagation Symp.*, Cranfield. p. 76 (1961).
4. H. D. WILLIAMS and G. C. SMITH, *Phil. Mag.* **13** (1966) 835.
5. M. J. MARCINKOWSKI, "Electron Microscopy and Strength of Crystals" (Interscience, New York, 1963) p. 333.
6. M. J. BLACKBURN, *Trans. AIME* **239** (1967) 660.
7. C. H. WELLS, *Acta Metalurgica* **17** (1969) 443.
8. R. W. HERTZBERG, Fatigue Crack Propagation, ASTM Special Technical publication 415, p. 205 (1967).
9. P. NEUMANN, *Acta Metallurgica* **17** (1969) 1219.
10. C. LAIRD, Fatigue Crack Propagation, ASTM Special Technical publication 415, p. 13 (1967).
11. HOEPNER, *ibid* p. 486.

Received 2 June and accepted 19 July 1970